Dynamic DNA Assemblies Mediated by Binding-Induced DNA Strand Displacement

Feng Li,[†] Hongquan Zhang,[‡] Zhixin Wang,[‡] Xukun Li,[†] Xing-Fang Li,[‡] and X. Chris Le*[,†,‡]

Departments of [†]Chemistry and [‡]Laboratory Medicine and Pathology, University of Alberta, Edmonton, Canada T6G 2G3

S *Supporting Information*

ABSTRACT: Dynamic DNA assemblies, including catalytic DNA circuits, DNA nanomachines, molecular translators, and reconfigurable nanostructures, have shown promising potential to regulate cell functions, deliver therapeutic reagents, and amplify detection signals for molecular diagnostics and imaging. However, such applications of dynamic DNA assembly systems have been limited to nucleic acids and a few small molecules, due to the limited approaches to trigger the DNA assemblies. Herein, we describe a binding-induced DNA strand displacement strategy that can convert protein binding to the release of a predesigned output DNA at room temperature with high conversion efficiency and low background. This strategy allows us to construct dynamic DNA assembly systems that are able to respond to specific protein binding, opening an opportunity to initiate dynamic DNA assembly by proteins.

Over the past 30 years, tremendous effort has contributed to the successful development of DNA nanostructures and nanodevices.[1] Attention has recently shifted from designing DNA nanostructures/devices to exploring their potential functions in biological systems, including regulating cell activities,[2] delivering therapeutic compounds,[3] and amplifying detection signals.[4] Successful applications of DNA assembly systems have been limited to nucleic acids and a few small molecules.[4b,h,5] It remains a challenge to apply DNA assembly systems to respond to specific proteins. We describe here a binding-induced DNA strand displacement strategy that uses proteins to initiate the process of diverse dynamic DNA assemblies.

Different from the toehold-mediated strand displacement which is currently the most widely used strategy to direct dynamic DNA assemblies,[6−8] the binding-induced DNA strand displacement strategy relies on protein binding to accelerate the rates of strand displacement reactions. Thus, the specific protein initiates the strand displacement process, and the displaced output DNA triggers dynamic DNA assemblies. To demonstrate this principle, we first show an isothermal binding-induced DNA strand displacement strategy that is able to release the predesigned output DNA at room temperature with high conversion efficiency and low background. We then apply this strategy to design two dynamic DNA assembly systems that are triggered by protein binding: a binding-induced DNA strand displacement beacon and a binding-induced DNA circuit.

Our strategy is illustrated in Figure 1. The binding-induced strand displacement strategy is designed to have target

Figure 1. Principle of the binding-induced DNA strand displacement strategy. Two DNA motifs (**OT** and **C**) are designed to bind to the same target molecule through a specific affinity ligand that is conjugated to the ends of both motifs. The **OT** motif is formed by prehybridizing the output DNA **O** with the supporting DNA **T**. Binding of the two affinity ligands to the same target molecule assembles two DNA motifs together, triggering an internal DNA strand displacement reaction between **OT** and **C**. As a result, **O** is released from **T**, and a subsequent dynamic DNA assembly can be initiated by the released **O**.

recognition and signal output elements. Target recognition is achieved by two specific affinity ligands binding to the same target molecule. One affinity ligand is conjugated to the output DNA motif (**OT**) that is formed by prehybridizing the output DNA (**O**) and the support DNA (**T**), and the other is conjugated to the competing DNA motif (**C**). The complementary sequence of **OT** was designed to have the same length as **C**. Thus, in the absence of the target molecule, the rate of the strand exchange reaction between **OT** and **C** is extremely slow at 25 °C.[9] However, in the presence of the target molecule, binding of the target molecule to the two affinity ligands that are linked to **OT** and **C** brings **C** in close proximity to **OT**. This process greatly increases the local concentration of **C** and accelerates the strand displacement reaction between **OT** and **C**. As a consequence, the output DNA **O** is released from its support **T**. The subsequent dynamic DNA assembly can be triggered by **O**, e.g., using the principle of toehold-mediated strand displacement. To be more specific, the toehold part of **O** is designed to be embedded in the complementary part of **OT** (Figure 1, black), so no dynamic DNA assembly can be triggered unless the target molecule is present and the toehold part of the output DNA is released.

We first designed a binding-induced strand displacement strategy for streptavidin using biotin as the affinity ligand (Figure S1). Streptavidin was selected for its extremely high binding affinity to biotin ($K_d = 10^{-14}$ M). This strong interaction ensures that the target binding process will not limit the performance of

the binding-induced strand displacement. **T** and **C** were each conjugated with a biotin molecule. The output **O** was designed to hybridize to **T** with a complementary length of 12 nt. **O** was extended with another 15 nt to help direct further DNA assemblies.

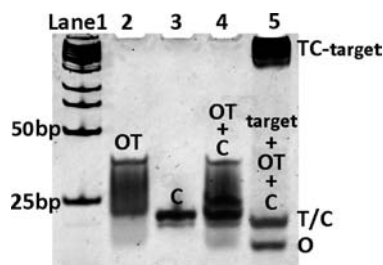Figure 2 shows the characterization of the relevant oligonucleotides using polyacrylamide gel electrophoresis

Figure 2. Native PAGE analysis of oligonucleotides from the binding-induced DNA strand displacement. Lane 1, low molecular DNA ladder; lane 2, 2 μM **OT**; lane 3, 2 μM **C**; lane 4, from analysis of a mixture containing 2 μM **OT** and 2 μM **C**; lane 5, from analysis of a mixture containing 2 μM **OT**, 2 μM **C**, and 1 μM streptavidin.

(PAGE). In the absence of the target streptavidin, the incubation of the two probes **OT** and **C** for 45 min does not lead to the release of **O** (Figure 2, lane 4), indicating that the rate of strand exchange between **OT** and **C** was extremely slow. However, in the presence of streptavidin, the observed strong bands of **O** and **TC**-target complex indicate the release of **O** from **OT** and the formation of **TC**-target complex according to Figure 1. These results suggest that the binding between streptavidin and biotin accelerated the kinetics of strand displacement reaction between **OT** and **C**.

As many dynamic DNA assembly systems, e.g., DNA catalytic circuits and nanomachines, use longer DNA molecules (e.g., 50 nt), we further tested the versatility of our strategy to output DNA of 50 nt (**L**) in length. As shown in Figure S2, a strong band of **L** appeared in lane 5 upon target binding, indicating that our strategy is applicable to release diverse output DNA molecules.

Having achieved isothermal binding-induced strand displacement, we further show that this strategy is able to direct dynamic DNA assemblies, using two examples: a strand displacement beacon[4d,7,8] and a catalytic DNA circuit.[4a−e] We first designed a toehold-mediated strand displacement beacon that was able to respond to the output DNA **O** (Figure 3A). Briefly, two complementary DNA strands are labeled with a fluorophore (**F**) and a quencher (**Q**), respectively. **Q** is designed to have 7 nt longer than **F**, which serves as a "toehold" for the hybridization of **Q** to the output DNA **O**. In the absence of **O**, a stable DNA duplex is formed between **F** and **Q**, and the fluorescence signal is quenched. However, in the presence of **O**, the toehold-mediated strand displacement reaction is initiated and **F** is released from **Q**, turning on the fluorescence signal (Figure S3). Thus, the binding-induced displacement beacon can be used to determine protein binding through monitoring of the displaced **O**.

Figure 3B shows the fluorescence signal increase of the binding-induced displacement beacon for streptavidin as a function of time. Within a period of 45 min, fluorescence intensities from 10 nM streptavidin (red curve) are readily distinguishable from the blank (green curve) that contained all reagents but not the target streptavidin. To confirm that the binding-induced displacement beacon is target specific, we tested our system using the same 10 nM streptavidin that was fully
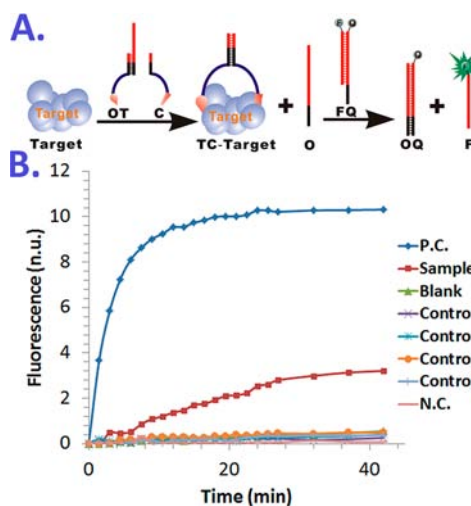

Figure 3. (A) Principle of the binding-induced strand displacement beacon. (B) Evaluation of the binding-induced displacement beacon. The fluorescence intensity was normalized such that 1 normalized unit (n.u.) corresponds to 1 nM **O**. Control-1 contained the same amount of streptavidin and reagents, except that 500 μM biotin was used to saturate all the binding sites of streptavidin. Control-2 was carried out using the same amount of streptavidin and reagents with the streptavidin sample solution, but without **O**. Similarly, Control-3 was carried out without competing DNA **C**, and Control-4 was carried out without **OT**. In the blank, all reagents were the same as in the streptavidin sample solution, except that there was no streptavidin. Positive control (P.C.), 10 nM **O**, 20 nM **FQ** in TE-Mg buffer; negative control (N.C.), only 20 nM **FQ** in TE-Mg buffer.

saturated with 500 μM of free biotin (Control-1). The results are similar to those of the blank. Likewise, in the absence of **O** (Control-2), **C** (Control-3), or **OT** (Control-4), only background fluorescence was detectable. These results suggest that specific binding is responsible for the fluorescence signals from the binding-induced displacement beacon.

Having established the binding-induced displacement beacon, we further estimated its efficiency of converting target streptavidin to the output DNA **O** (details in Supporting Information (SI) and Figure S4) at different target concentrations. By comparing the experimentally determined concentrations of **O** with their theoretical concentrations, we found that the average converting efficiency was 99.3 ± 7.6% throughout a wide range of target concentrations (160 pM to 10 nM) (Figure 4).

To demonstrate the general applicability of our strategy, we applied the binding-induced displacement beacon to the analysis of a clinically relevant protein, platelet derived growth factor (PDGF). A DNA aptamer for PDGF-BB was incorporated into the DNA probes **OT** and **C**, forming **Apt-OT** and **Apt-C** (Table S2). Binding of PDGF-BB to its aptamer sequences in **OT** and **C** brought the two DNA probes together, resulting in the displacement of output DNA **O** (Figure S6A). The released output DNA **O** triggered a subsequent toehold-mediated strand displacement reaction, releasing **F** from **FQ**. Fluorescence intensity from **F** provided a measure for the detection of PDGF-BB. The fluorescence intensity increases with the increase of PDGF concentration (Figure S6B). These quantitative results demonstrate an application of the binding-induced strand displacement beacon to the detection of PDGF protein.

The success of binding-induced displacement beacon opens up opportunities for directing further dynamic DNA assemblies,
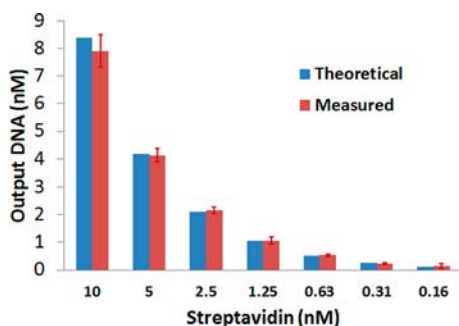
Figure 4. Estimation of the conversion efficiency from target streptavidin to **O** at different streptavidin concentrations through the binding-induced displacement beacon. The streptavidin test solutions contained 20 nM **OT**, 20 nM **C**, 20 nM **QF**, and varying concentrations of streptavidin. Error bars represent one standard deviation from duplicate analyses.

e.g., catalytic DNA circuit.[4a−c] Because these DNA assemblies of higher structural complexity often require extended periods of incubation, it is critical to minimize the background that can also be amplified over the extended periods (Figure 5B). Thus, we
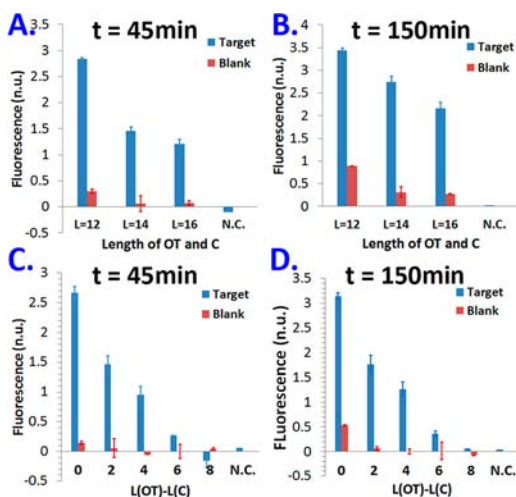

Figure 5. Optimization of the binding-induced DNA strand displacement to minimize the target-independent strand displacement. Streptavidin test solutions contained 5 nM streptavidin, 10 nM **OT**, 10 nM **C**, and 20 nM **FQ**. In the blank, all reagents were the same as streptavidin sample solution, but with no streptavidin added. Effects of simultaneous increases in the length of both **OT** and **C** on the performance of the binding-induced strand displacement were monitored at 45 (A) and 150 min (B). Effects of the length difference between **OT** and **C** were also monitored at 45 (C) and 150 min (D). The negative control (N.C.) contained only 20 nM **FQ** in TE-Mg buffer. Error bars represent one standard deviation from duplicated analyses.

have optimized the designs of oligonucleotides, **OT** and **C**, to minimize target-independent strand displacement. This optimization is based on the previous discovery that increasing the length of DNA duplex could slow down the rate of strand exchange reactions drastically.[9]

As shown in Figure 5A,B, in the presence of 10 nM streptavidin, the fluorescence intensities decrease with increasing length of **OT** and **C** from 12 to 16 nt. An extended incubation period (e.g., 150 min) results in noticeable increases in background (Figure 5B), suggesting the target-independent displacement of output DNA **O**. To eliminate the target-

independent displacement, we fixed the competing DNA **C** to be 12 nt in length, and increased the length of **OT** from 12 to 20 nt. In principle, shorter competing DNA is thermodynamically unfavored to displace a longer DNA strand, and thus should be able to suppress nonspecific release of **O**. Indeed, Figure 5C,D shows that the nonspecific displacement can be eliminated even after incubation for 150 min. To maximize signal-to-background, we chose a 2-nt difference between **OT** (14 nt) and **C** (12 nt). We also examined this optimized condition with PAGE (Figure S7), and found that no output DNA **O** band was observed on the gel without target molecule (lane 4), while a strong **O** band appeared with target (lane 5). These results confirm that we are able to eliminate the target-independent displacement of output DNA **O**.

Upon eliminating the target-independent displacement, we further designed a binding-induced catalytic DNA circuit to demonstrate the ability of our strategy to direct dynamic DNA assemblies with higher structural complexity. The principle of our binding-induced catalytic DNA circuit strategy is shown in Figure 6A: a pair of DNA hairpins (**H1** and **H2**) is designed to
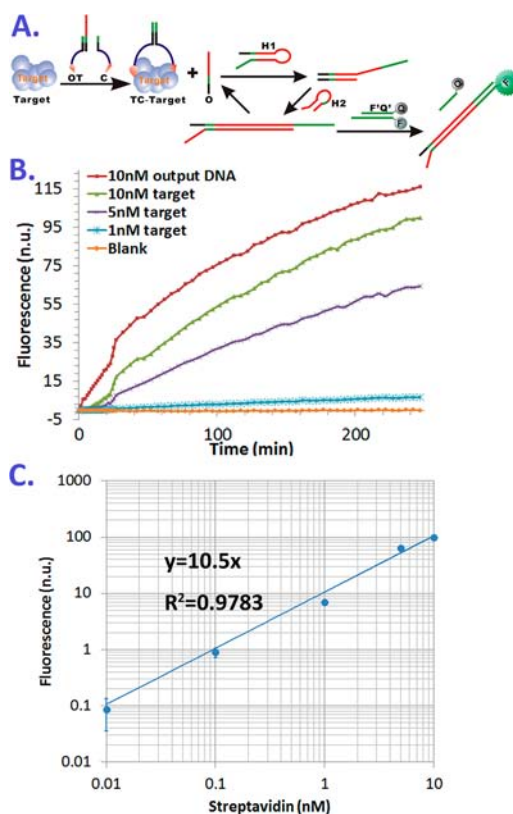

Figure 6. (A) Principle of the binding-induced catalytic DNA circuit. (B) Evaluation of the binding-induced catalytic DNA circuit. The fluorescence intensity was normalized such that 1 n.u. corresponds to 1 nM positive DNA **P** (details in the SI). An output DNA test solution contained 10 nM output DNA **O**, 125 nM **H1**, 200 nM **H2**, and 125 nM **F′Q′**. Streptavidin test solutions contained 20 nM **OT**, 20 nM **C**, 125 nM **H1**, 200 nM **H2**, 125 nM **F′Q′**, and varying concentrations of streptavidin. In the blank, all reagents were the same as in the streptavidin test solutions, but without streptavidin. (C) Increases in fluorescence intensity reflect increasing concentrations of streptavidin that converts to positive DNA **P** by the binding-induced catalytic DNA circuit. The magnitude of amplification was determined by the linear fitting between fluorescence intensity and concentration of streptavidin. Error bars represent one standard deviation from duplicated analyses.

partially hybridize to each other. However, the spontaneous hybridization between **H1** and **H2** is kinetically hindered by caging complementary regions in the stems of the hairpins. In the presence of the target molecule, the output DNA **O** is released by the binding-induced strand displacement reaction. The released output DNA opens the stem part of **H1** by the principle of the toehold-mediated DNA strand displacement. The newly exposed sticky end of **H1** nucleates at the sticky end of **H2** and triggers another strand-displacement reaction to release **O**. Thus, **O** is able to act as a catalyst to trigger the formation of other **H1-H2** complexes. This process results in amplification of the detection signals.

To test the signal amplification ability of our binding-induced DNA circuit, we monitored the fluorescence intensity increase as a function of time over a period of 4 h. As shown in Figure 6B, the fluorescence intensity generated from 10 nM streptavidin is close to 100 normalized units, which corresponds to 100 nM positive DNA (**P**) (Figure S8). Essentially no background fluorescence signal was observed for the blank. Compared to the toehold-mediated catalytic DNA circuit that is triggered directly by the output DNA **O** (Figure 6B, red curve), the binding-induced catalytic DNA circuit (Figure 6B, green curve) demonstrates comparable signal amplification capability. Furthermore, the measured fluorescence intensities are responsive to the concentrations of streptavidin in the range of 10 pM to 10 nM (Figure 6C), demonstrating the capability for quantification. We estimated from the standard curve (Figure 6C) that the fluorescence signal has been amplified by over 10-fold throughout this concentration range.

In conclusion, we have successfully developed a binding-induced DNA strand displacement strategy that functions at room temperature with high conversion efficiency and low background. Our success in constructing the binding-induced displacement beacon and binding-induced catalytic DNA circuit has demonstrated the feasibility of our strategy to direct dynamic DNA assemblies that are able to respond to protein binding. The concept and strategies have potential to further expand the existing dynamic DNA nanotechnology to proteins for diverse applications. One such application could be in the area of point-of-care analysis of proteins that could be performed under ambient temperature and without requiring the use of enzymes for signal generation and/or amplification. It is necessary to have the DNA strand displacement process faster than the dissociation of the target from affinity ligands. This requirement can be achieved by using affinity ligands with slow dissociation rate, e.g., slow off-rate modified aptamer (SOMAmer);[10] stabilizing the binding complex by photo or chemical cross-linking;[11] and/or increasing the rate of intramolecular DNA strand displacement by tuning the length of DNA probes or increasing the incubation temperature.[12]

As has been shown in proximity ligation assays and binding-induced DNA assembly assays,[12,13] diverse affinity ligands, including antibodies, peptides, and aptamers, can be conjugated to DNA probes and form affinity complexes with target molecules, thereby triggering DNA assemblies. We anticipate that our strategy can also be applied to studies of molecular interactions, e.g., protein-protein and DNA-protein interactions.

■ ASSOCIATED CONTENT

ⓢ Supporting Information

Supporting figures, DNA sequences, and detailed experimental methods. This material is available free of charge via the Internet at http://pubs.acs.org.

■ AUTHOR INFORMATION

Corresponding Author
xc.le@ualberta.ca

Notes
The authors declare no competing financial interest.

■ REFERENCES

(1) (a) Seeman, N. C. *J. Theor. Biol.* **1982**, *99*, 237. (b) Winfree, E.; Liu, F.; Wenzler, L. A.; Seeman, N. C. *Nature* **1998**, *394*, 539. (c) Aldaye, F. A.; Palmer, A. L.; Sleiman, H. F. *Science* **2008**, *321*, 1795. (d) Douglas, S. M.; Dietz, H.; Liedl, T.; Hogberg, B.; Graf, F.; Shih, W. M. *Nature* **2009**, *459*, 414. (e) Wei, B.; Dai, M.; Yin, P. *Nature* **2012**, *485*, 623. (f) Zhang, D. Y.; Seelig, G. *Nat. Chem* **2011**, *3*, 103. (g) Pinheiro, A. V.; Han, D.; Shih, W. M.; Yan, H. *Nat. Nanotechnol.* **2011**, *6*, 763. (h) Wang, Z.; Tang, L.; Tan, L. H.; Li, J.; Lu, Y. *Angew. Chem., Int. Ed.* **2012**, *51*, 9078.

(2) Venkataraman, S.; Dirks, R. M.; Ueda, C. T.; Pierce, N. A. *Proc. Natl. Acad. Sci. U.S.A.* **2010**, *107*, 16777.

(3) (a) Douglas, S. M.; Bachelet, I.; Church, G. M. *Science* **2012**, *335*, 831. (b) Jiang, Q.; Song, C.; Nangreave, J.; Liu, X.; Lin, L.; Qiu, D.; Wang, Z.-G.; Zou, G.; Liang, X.; Yan, H.; Ding, B. *J. Am. Chem. Soc.* **2012**, *134*, 13396.

(4) (a) Yin, P.; Choi, H. M. T.; Calvert, C. R.; Pierce, N. A. *Nature* **2008**, *451*, 318. (b) Li, B.; Ellington, A. D.; Chen, X. *Nucleic Acids Res.* **2011**, *39*, e110. (c) Qian, L.; Winfree, E. *Science* **2011**, *332*, 1196. (d) Li, B.; Jiang, Y.; Chen, X.; Ellington, A. D. *J. Am. Chem. Soc.* **2012**, *134*, 13918. (e) Li, B.; Chen, X.; Ellington, A. D. *Anal. Chem.* **2012**, *84*, 8371. (f) Picuri, J. M.; Frezz, B. M.; Ghadiri, M. R. *J. Am. Chem. Soc.* **2009**, *131*, 9368. (g) Liao, S.; Seeman, N. C. *Science* **2004**, *306*, 2072. (h) Surana, S.; Bhat, J. M.; Koushika, S. P.; Krishnan, Y. *Nat. Commun.* **2011**, *2*, 340. (i) Modi, S.; Swetha, M. G.; Goswami, D.; Gupta, G. D.; Mayor, S.; Krishnan, Y. *Nat. Nanotechnol.* **2009**, *4*, 325. (j) Seferos, D. S.; Giljohann, D. A.; Hill, H. D.; Prigodich, A. E.; Mrikin, C. A. *J. Am. Chem. Soc.* **2007**, *129*, 15477. (k) Lin, C.; Liu, Y.; Yan, H. *Nano Lett.* **2007**, *7*, 507. (l) Pei, H.; Liang, L.; Yao, G.; Li, J.; Huang, Q.; Fan, C. *Angew. Chem., Int. Ed.* **2012**, *51*, 9020. (m) Liu, H.; Xiang, Y.; Lu, Y.; Crooks, R. M. *Angew. Chem., Int. Ed.* **2012**, *51*, 6925. (n) El-Hamed, F.; Dave, N.; Liu, J. *Nanotechnology* **2012**, *22*, 494011.

(5) (a) Xing, Y.; Yang, Z.; Liu, D. *Angew. Chem., Int. Ed.* **2011**, *50*, 11934. (b) Dirks, R. M.; Pierce, N. A. *Proc. Natl. Acad. Sci. U.S.A.* **2004**, *101*, 15275. (c) Zhang, D.; Seferos, D. S.; Giljohann, D. A.; Patel, P. C.; Mirkin, C. A. *Nano Lett.* **2009**, *9*, 3258.

(6) (a) Zhang, D. Y.; Winfree, E. *J. Am. Chem. Soc.* **2009**, *131*, 9368. (b) Genot, A. J.; Zhang, D. Y.; Bath, J.; Turberfield, A. J. *J. Am. Chem. Soc.* **2011**, *133*, 2177. (c) Chen, X. *J. Am. Chem. Soc.* **2012**, *134*, 263.

(7) Li, Q.; Luan, G.; Guo, Q.; Liang, J. *Nucleic Acids Res.* **2002**, *30*, e5.

(8) Zhang, D. Y.; Chen, S. X.; Yin, P. *Nat. Chem* **2012**, *4*, 208.

(9) Reynaldo, L. P.; Vologodskii, A. V.; Neri, B. P. *J. Mol. Biol.* **2000**, *297*, 511.

(10) Gold, L.; Ayers, D.; Bertino, J.; et al. *PLoS One* **2010**, *5*, e15004.

(11) Vinkenborg, J. L.; Mayer, G.; Famulok, M. *Angew. Chem., Int. Ed.* **2012**, *51*, 9176.

(12) Li, F.; Zhang, H.; Lai, C.; Li, X.-F.; Le, X. C. *Angew. Chem., Int. Ed.* **2012**, *51*, 9317.

(13) (a) Fredriksson, S.; Gullberg, M.; Jarvius, J.; Olsson, C.; Pietra, K.; Gustafsdottir, S. M.; Ostman, A.; Landegren, U. *Nat. Biotechnol.* **2002**, *20*, 473. (b) Heyduk, E.; Dummit, B.; Chang, Y.-H.; Heyduk, T. *Anal. Chem.* **2008**, *80*, 5152. (c) Zhang, H.; Li, X.-F.; Le, X. C. *Anal. Chem.* **2012**, *84*, 877.